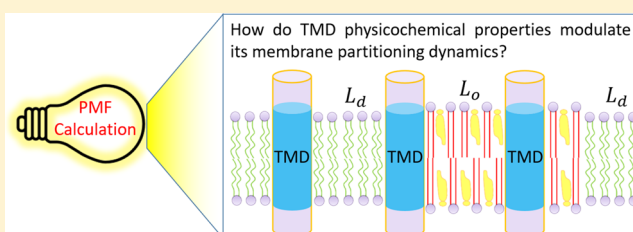


Understanding Membrane Domain-Partitioning Thermodynamics of Transmembrane Domains with Potential of Mean Force Calculations

Xubo Lin^{*,†,‡,§} and Alemayehu A. Gorfe^{*,‡,§}[†]Beijing Advanced Innovation Center for Biomedical Engineering, Beihang University, Beijing 100083, China[‡]Key Laboratory of Ministry of Education for Biomechanics and Mechanobiology, School of Biological Science and Medical Engineering, Beihang University, Beijing 100083, China[§]Department of Integrative Biology and Pharmacology, McGovern Medical School, The University of Texas Health Science Center at Houston, Houston, Texas 77030, United States

S Supporting Information

ABSTRACT: The transmembrane domain (TMD) of membrane proteins plays an essential role in their dynamics and functions. Certain properties of TMDs, such as raft affinity and orientation, have been studied extensively both experimentally and computationally. However, the extent to which specific physicochemical properties of TMDs determine their membrane domain-partitioning thermodynamics is still far from clear. In this work, we propose an approach based on umbrella sampling molecular dynamics simulations of model membranes and idealized TMDs to quantify the effect of TMD physicochemical properties, namely, length, degree of hydrophobicity, and size of TMDs, on their membrane domain-partitioning thermodynamics. The results, which are fully consistent with previous experimental and simulation data, indicate that the concept of “hydrophobic mismatch” should go beyond differences in hydrophobic thickness to include mismatch in the degree of hydrophobicity between the TMD and the surrounding hydrocarbon lipid chains. Our method provides quantitative insights into the role of specific physicochemical features of TMDs in membrane localization and orientation, which will be broadly useful for predicting the raft affinity and membrane partitioning of any transmembrane protein.



INTRODUCTION

The plasma membrane plays critical roles in maintaining the complex functions of the cell.¹ In addition to being the first biological barrier of mammalian cells, it provides a versatile platform for proteins and lipids to participate in various biological processes, including signal transduction and trafficking of substances. The dynamics of membrane proteins and lipids is important in regulating these processes. The plasma membrane is functionally and compositionally segregated into distinct nanoscale domains with different biophysical properties. These include “raft” and “nonraft” domains^{2,3} that have been widely studied both with experiments and simulations using model membranes.^{4–10} These studies have revealed that the domain preference of membrane proteins determines their clustering, dynamics, and subcellular localization. Hence, many efforts have been made to understand the raft affinity of mammalian membrane proteins.^{11–13} However, the factors that determine domain preferences of transmembrane proteins are still far from clear. For example, there are more than 500 crystal structures of transmembrane proteins in the Protein Data Bank,^{14,15} but no universally applicable relationship between the physicochemical properties of transmembrane proteins and their membrane partitioning thermodynamics has been established.

Single-pass transmembrane peptides are useful models to study transmembrane proteins and are therefore widely used both in experiments^{10,12,16,17} and simulations.^{13,18,19} With the help of such simplified models, increasingly deeper insights have been gained into the raft affinity of transmembrane proteins. For example, the transmembrane domain (TMD) hydrophobic length has been shown to affect raft affinity.^{10,20,21} In addition, lipid modifications of TMDs, including palmitoylation^{16,17} and glycosylphosphatidylinositol modification,^{8,22} can significantly enhance raft affinity by promoting interactions with raft lipids.²³ Most recently, the surface area of TMDs was also found to be important for membrane domain-partitioning.¹² However, it is still not easy to differentiate the specific role of each physicochemical property of a TMD to its raft affinity because each of the key factors mentioned above have contributions from multiple physicochemical properties. For example, when lipid modifications are introduced to TMDs, both the hydrophobicity and size of the TMD change. If the contribution of a specific physicochemical property of a TMD to raft affinity is known, one can predict the raft affinity of any TMD.

Received: October 17, 2018

Revised: January 12, 2019

Published: January 14, 2019

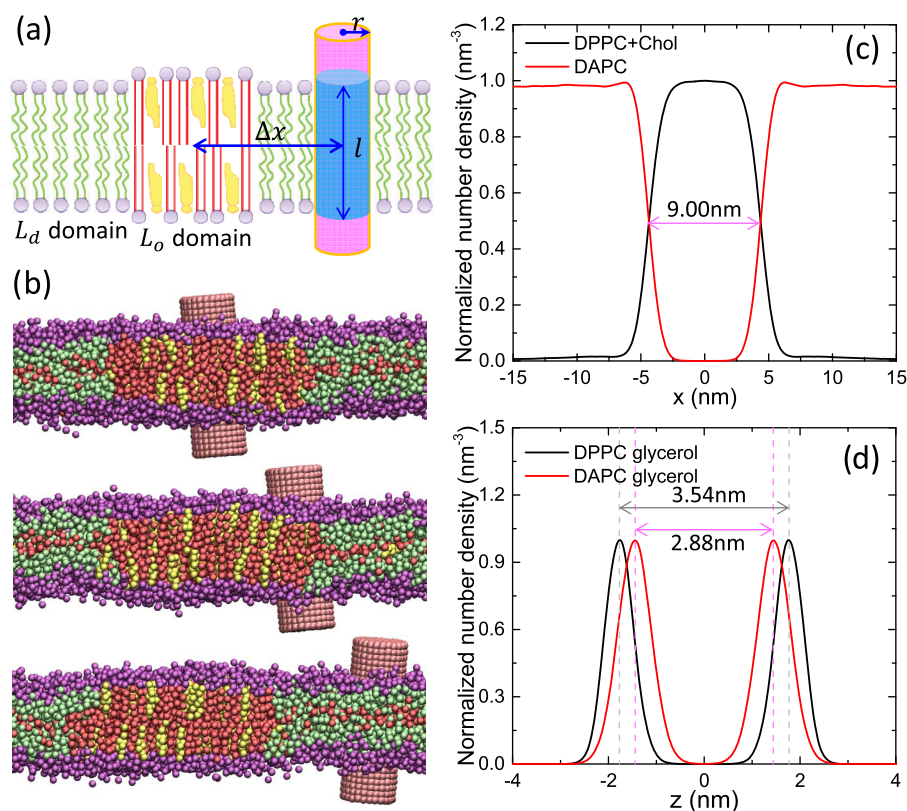


Figure 1. (a) Schematic of the system used for PMF calculations: r and l are the radius and hydrophobic length of the idealized TMD, respectively, and the center-of-mass (COM) distance along the x -axis (Δx) between the TMD and the L_o domain is used as the reaction coordinate for umbrella sampling. (b) Initial system configurations with the TMD placed in the L_o domain (top), the interface (middle), and the L_d domain (bottom). The head-group of the PC lipids is shown in purple, and lipid tail beads are in red for saturated acyl chains and in lime for unsaturated acyl chains. The hydrophilic section of the TMD is in pink, and the hydrophobic part in cyan. For clarity, only membrane and TMD are shown. (c) Normalized number density along the x -axis for the L_o and L_d domain lipids, indicating that the x -width of the L_o domain is about 9 nm. (d) Normalized number density along the z -axis (membrane normal) for DPPC and DAPC glycerol groups shows that the average hydrophobic thicknesses of L_o and L_d domains are 3.54 and 2.88 nm, respectively.

In this work, we characterized the specific roles of the TMD hydrophobic length, hydrophobicity, and size in determining raft affinity using idealized TMD models and potential of mean force (PMF) calculations with molecular dynamics (MD) simulations. Idealized TMDs, in which the physicochemical properties can be systematically varied, can provide insights into the relative roles of the TMD length, hydrophobicity, and size in raft affinity and have been used as a standard physical model to study TMD dynamics in model membrane systems.^{24–27} In other words, studies of idealized TMDs will enable us to separately characterize the specific role of a given TMD property in determining the membrane partitioning thermodynamics of a real transmembrane protein (e.g., TMD of linker for the activation of T cell receptor¹³). Similarly, PMF calculations have been used to gain insights into the thermodynamics of many biological processes, such as dimerization of transmembrane proteins²⁸ and translocation of small molecules across lipid membranes.^{29,30}

METHODS

Choice of the Model Membrane and Idealized TMDs for PMF Calculations. Coarse-grained (CG) MD simulations have been widely used to study membrane proteins and lipid rafts.^{6,31} In the current study, we used the Martini CG model³² of lipids, which maps on average four heavy atoms into one interaction site.³² We chose a lipid bilayer made up of 1,2-

dipalmitoyl-*sn*-glycero-3-phosphocholine (DPPC), 1,2-diarachidonoyl-*sn*-glycero-3-phosphocholine (DAPC), and cholesterol (Chol), which forms very stable membrane domains,⁶ to test the feasibility of our approach to quantify TMD raft affinity.

To construct idealized TMD models with tunable physicochemical puppetries, we adapted the standard Martini CG force field for proteins as follows: (1) evenly placed beads were stacked up with a minimum distance of 0.3 nm to form a “cylinder”; (2) a CG parameter of type “Q0” was assigned to beads at the two ends of the cylinder (length: 2 nm) to model the two hydrophilic termini of the TMD, and parameters of type “C1” or “C5” were assigned to beads in the middle of the cylinder to simulate a TMD segment with different hydrophobicity (C1 is more hydrophobic); and (3) beads within 1 nm distance were constrained (force constant: 1250 kJ mol⁻¹ nm⁻¹) to obtain a rigid, idealized TMD. Such an idealized TMD enabled us to tune any physicochemical property during the simulations. Thus, we studied the effect of three properties of TMDs on the lateral dynamics of single-pass transmembrane helices across membrane domains: hydrophobic length ($l = 2, 3, 4, 5$ nm), radius ($r = 0.6, 1.2$ nm), and hydrophobicity (“C1”, more hydrophobic; “C5”, less hydrophobic). To conduct the simulations with different l , r , and C values, we first built a membrane model with an L_o domain in the middle flanked by two L_d domains (Figure 1a,b). The width of the L_o

Table 1. Summary of the PMF Calculations Conducted in This Work

system	TMD			membrane composition	membrane undulation removal	duration (μs)
	radius (r , nm)	hydrophobicity	hydrophobic length (l , nm)			
1	0.6	C1	2	DPPC/Chol/DAPC	yes	51 × 1
2	0.6	C1	3	DPPC/Chol/DAPC	yes	51 × 1
3	0.6	C1	4	DPPC/Chol/DAPC	yes	51 × 1
4	0.6	C1	5	DPPC/Chol/DAPC	yes	51 × 1
5	0.6	C5	2	DPPC/Chol/DAPC	yes	51 × 1
6	0.6	C5	3	DPPC/Chol/DAPC	yes	51 × 1
7	0.6	C5	4	DPPC/Chol/DAPC	yes	51 × 1
8	0.6	C5	5	DPPC/Chol/DAPC	yes	51 × 1
9	1.2	C1	2	DPPC/Chol/DAPC	yes	51 × 1
10	1.2	C1	3	DPPC/Chol/DAPC	yes	51 × 1
11	1.2	C1	4	DPPC/Chol/DAPC	yes	51 × 1
12	1.2	C1	5	DPPC/Chol/DAPC	yes	51 × 1
13	1.2	C5	2	DPPC/Chol/DAPC	yes	51 × 1
14	1.2	C5	3	DPPC/Chol/DAPC	yes	51 × 1
15	1.2	C5	4	DPPC/Chol/DAPC	yes	51 × 1
16	1.2	C5	5	DPPC/Chol/DAPC	yes	51 × 1
17	0.6	C1	4	DPPC/Chol/DAPC	no	51 × 1
18	0.6 ^a	C1 ^a	4 ^a	DPPC/Chol/DAPC	yes	51 × 1
19	0.6 ^b	C1 ^b	4 ^b	DPPC/Chol/DAPC	yes	51 × 1
20	0.6	C1	4	DPPC/Chol/DUPC	yes	51 × 1

^aInteractions between CG beads within the TMD are reduced to mimic a flexible TMD with a relatively rough surface. ^bCG beads packed loosely (minimum distance: 0.5 nm; this value is 0.3 nm for the rest of the simulations). Since “C1” is more polar than “C5”, as defined in the Martini CG model, the two beads represent different hydrophobicities. The membrane is composed of 360 DPPC, 180 Chol, and 712 DAPC or 1,2-dilinoleoyl-*sn*-glycero-3-phosphocholine (DUPC) molecules.

domain along the x -axis (i.e., the direction of our reaction coordinate Δx) is ~ 9 nm (see Figure 1c), whereas its hydrophobic thickness is 3.54 nm, greater than the 2.88 nm hydrophobic thickness of the L_d domain (Figure 1d). Second, idealized TMDs characterized by the various l , r , and C values listed above were placed at different locations to obtain different initial configurations for umbrella sampling simulations (Figure 1b). For each TMD, we performed 51 independent simulations at different Δx values spanning the L_o and L_d domains as well as the interface between them.

Umbrella Sampling Simulations. The relative free energy ΔG of a process along a reaction coordinate can be calculated by umbrella sampling simulations³³ using $\frac{\partial}{\partial \xi} \Delta G = -\langle F_\xi \rangle_\xi$, where F_ξ is the force along the reaction coordinate ξ . To quantify the raft affinity of TMDs, we first generated a phase-separated model membrane with a stripped L_o domain enriched with DPPC and Chol at the center flanked by two L_d domains enriched with DAPC. The center-of-mass (COM) distance (Δx , Figure 1a) between the TMD and the L_o domain along the x -axis (i.e., perpendicular to the membrane normal) was chosen as the reaction coordinate. A total of 51 independent simulations with window size of 0.2 nm were performed for each TMD model.

Simulations were performed using GROMACS 5.0.4³⁴ with the Lennard–Jones potential smoothly shifted to zero between 1.0 and 1.4 nm. Electrostatic interactions were calculated using the Coulombic potential with a smooth shift from 0 to 1.4 nm. The default relative dielectric constant of 15 was used.³² TMDs, lipids, water, and ions were coupled separately to V -rescale heat baths³⁵ at $T = 310$ K (coupling constant $\tau = 1$ ps). The systems were simulated at 1 bar using a semi-isotropic Parrinello–Rahman pressure coupling scheme³⁶ with a coupling constant (τ) of 4 ps and compressibility of 4 ×

10^{-5} bar⁻¹. The nonbonded neighbor list was updated every 10 steps with a cutoff of 1.4 nm. Using the pull code in GROMACS³⁴ to maintain reaction coordinate Δx , each simulation was run for 1 μs with a time step of 20 fs and the last 800 ns data was used for analysis. Physical simulation time was used here, and the corresponding effective time can be estimated by multiplying by a factor of 4.³² In summary, 16 different TMD models as well as 4 reference systems were studied with umbrella sampling MD simulations using the Martini CG model, with the total simulation time being 20 × 51 × 1 $\mu\text{s} = 1020$ μs (Table 1).

RESULTS AND DISCUSSION

CGMD simulations have been used previously to study the lateral dynamics of transmembrane helices in model membranes.¹⁸ However, the free energy of partitioning across the interface between liquid-ordered (L_o or raft) and liquid-disordered (L_d or nonraft) domains has rarely been quantified. Our goal here is to reveal the free energy landscape for the lateral dynamics of TMDs across L_o and L_d domains using PMF calculations with umbrella sampling MD of the simplified model TMDs. In umbrella sampling, the reaction coordinate needs to be a continuous parameter. The uniqueness of our reaction coordinate Δx can be affected by the stability of the membrane domains or membrane undulation. To mitigate the former, we chose a DPPC/DAPC/Chol bilayer system where the L_o and L_d domains are much more stable⁶ than those in the widely used DPPC/DUPC/Chol mixture.^{7,18,31} We prevented membrane undulation by adding a small position restraint ($k = 2$ kJ mol⁻¹ nm⁻¹) along the z -axis on one glycerol bead of each DPPC and DAPC molecule in one leaflet; this restraint has little effect on other membrane properties, as shown by Ingólfsson et al.³⁷ Using this construct, we studied the effect of three different properties of TMDs on the movement of

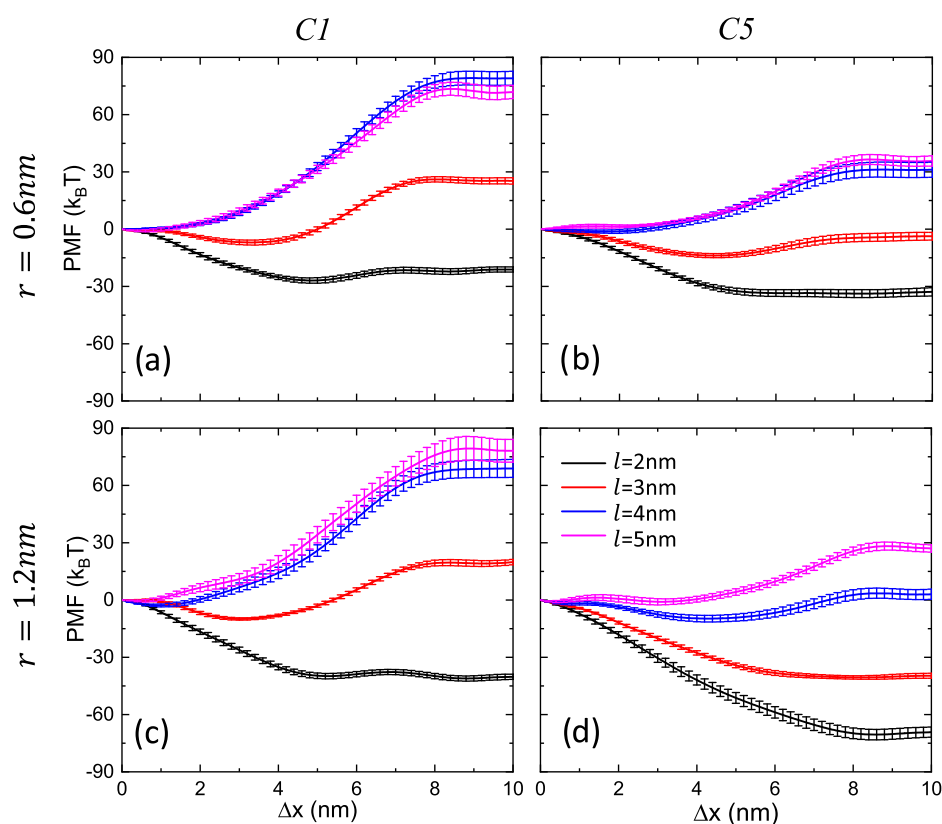


Figure 2. PMF profiles of membrane domain partitioning of TMDs with different physicochemical properties. $\Delta x < 4.5$ nm corresponds to the L_o domain, whereas $4.5 \text{ nm} \leq \Delta x \leq 10$ nm represents the L_d domain. For each TMD, 51 independent umbrella sampling simulations, each of length $1 \mu\text{s}$, were performed to obtain the PMF profile. Error bars are standard deviations based on statistics from eight 100 ns blocks over last 800 ns of the trajectory and are drawn as lines with caps. C1 and C5 denote the different degree of hydrophobicity of the TMDs in the left and right panels, respectively. TMDs in panels (a) and (b) have a radius of 0.6 nm, and those in panels (c) and (d) are have a radius of 1.2 nm.

proteins across membrane domains: hydrophobic length (l), hydrophobicity (C), and size or radius (r) of TMDs; the abundant experimental data on some of these properties, such as l , allowed us to make direct comparison with experiments and validate our predictions.

Effect of TMD Physicochemical Properties on Raft Affinity. We performed a series of umbrella sampling MD simulations to obtain potential of mean force (PMF) profiles of our model TMDs with various physicochemical properties. As shown in Figure 2, the location of the free energy minimum varies with l , r , and C of the TMD and can be found at the bulk L_o domain, the domain interface, or the bulk L_d domain. In subsequent paragraphs, we discuss the role of the hydrophobic length, hydrophobicity, and size in TMD membrane partitioning thermodynamics.

Numerous experimental studies have shown that the hydrophobic mismatch between a TMD and its host membrane plays an important role in determining domain preference.^{10,20,21,38,39} Since the hydrophobic thickness of the L_o domain is typically larger than that of the L_d domain, TMDs with longer hydrophobic length tend to have higher raft affinity. In our model membrane, the hydrophobic thicknesses of the L_o and L_d domains are 3.54 and 2.88 nm, respectively. Due to hydrophobic mismatch, our TMDs of hydrophobic lengths $l = 2, 3, 4, 5$ nm are expected to have different preferences for L_o and L_d domains. As shown in each panel of Figure 2, TMDs with the shortest hydrophobic length ($l = 2$ nm) are always excluded from the L_o domain. When increasing the hydrophobic length, the energy barrier for TMDs crossing

into the bulk L_o domain gets smaller and smaller or even becomes negative. In other words, the raft affinity increases with the TMD hydrophobic length. Our free energy profiles (Figure 2) show the role of TMD hydrophobic length in determining raft affinity, consistent with experiments.^{10,20,21,38,39} It is worth mentioning that there are several examples in Figure 2 where the energy minimum is at the domain interface, which is consistent with our previous MD simulations of the transmembrane LAT peptide (linker for activation of T cell receptors).¹³ The agreement between the current results and previous reports from experiments and simulations on the role of hydrophobic length on lipid domain preference of TMDs provides a strong support for the viability of our approach, namely, calculation of free energy profiles using simplified model systems to quantify the roles of TMD physical and chemical properties on domain preference.

In addition to length, variations in hydrophobicity and radius of TMDs arising from variations in hydrophobicity and size of protein side chains^{38,39} will likely affect lateral dynamics of transmembrane proteins. However, precisely how and to what extent these two factors regulate raft affinity is far from clear. Our calculations provide insights into this issue. Comparison of the free energy profiles of TMDs harboring more hydrophobic C1 beads (Figure 2, left panels) with those made up of the less hydrophobic C5 beads (Figure 2, right panels) clearly shows that changes in TMD hydrophobicity significantly alter raft affinity. More hydrophobic TMDs tend to partition into the raft domain more easily. This is consistent with the liquid phase separation of lipids, which is partially

driven by differences in the hydrophobicity of lipid acyl chains.^{23,40–42} Such differences in hydrophobicity between raft and nonraft lipids mean that TMDs of different hydrophobicity would have different raft affinities. In other words, the phrase “hydrophobic mismatch” should include mismatch of TMD hydrophobic length and hydrophobicity.

As shown in Figure 2, the effect of TMD size (i.e., radius r) on raft affinity is less significant when the TMD is either highly hydrophobic (C1) or very long and therefore already “raftophilic”. This means that the effect of helical radius can be relatively small when there is a large mismatch in hydrophobicity or length. However, in other cases, raft affinity generally decreases with TMD size. For example, TMDs with hydrophobic length $l = 3$ nm and hydrophobicity C5 have totally different raft affinity when $r = 1.2$ or 0.6 nm. The thinner TMD ($r = 0.6$ nm) exhibits similar preferences to both raft and nonraft domains, whereas the larger TMD ($r = 1.2$ nm) shows complete nonraft affinity, where much higher energy barrier induced by the TMD size makes it impossible to cross into the raft domain. It is worth mentioning that the role of TMD size in raft affinity observed here is consistent with our recent experimental results on the role of TMD surface area.¹²

The qualitative agreement of our PMF calculations with previously reported results provides support for the usefulness of our approach to predict the raft affinity of transmembrane proteins. However, the free energy differences between lipid domains (tens of $k_B T$) suggested by our PMF calculations are much larger than those obtained from experiments.^{10,12,17} An obvious explanation is the difference between the simulations and experiments in lipid composition. However, other contributing factors should also be considered. As mentioned above, we used a weak position restraint ($k = 2$ kJ mol⁻¹ nm⁻¹) along the z -axis on one glycerol bead of DPPC and DAPC molecules on one membrane leaflet to remove membrane undulation. Previous studies indicated that this treatment had a negligible effect on lipid organization.³⁷ Consistent with this observation, removing the restraint and allowing membrane undulation (Figure S1f–i) had no significant effect on the PMF profile of our model systems (compare control and free membrane in Figure 3). In addition, our idealized TMDs are

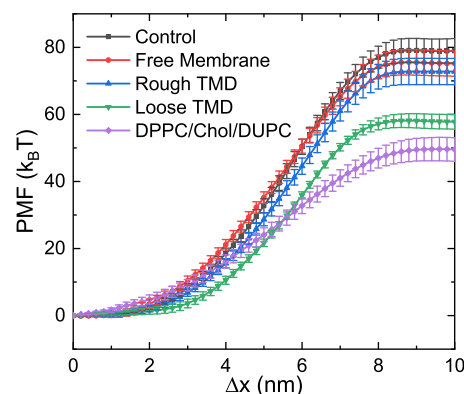


Figure 3. Free energy profile of a TMD in a DPPC/Chol/DAPC bilayer simulated without a restraint force to remove membrane undulation (free membrane), modeled with increased surface roughness (rough TMD) or decreased packing density (loose TMD), and simulated in a membrane model with lower domain stability (DPPC/Chol/DUPC). A DPPC/Chol/DAPC membrane system containing a TMD of radius $r = 0.6$ nm, hydrophobicity C5, and hydrophobic length $l = 4$ nm was used as the reference (control).

packed relatively densely (minimum distance of 0.3 nm) and are kept rigid and thus have a smooth surface. We tested the possible effect of these two simplifications on the PMF profiles by respectively decreasing the packing density and increasing the surface roughness of a TMD model. As shown in Figure 3, the free energy difference between ordered and disordered domains significantly reduced when we replace the initial TMD with a less dense TMD (Figure S1a,c). We also tested the effect of the restraint among the CG beads within our idealized TMD by reducing the force constant to obtain a relatively flexible and rough TMD (Figure S1a,b). We found that surface roughness can also contribute to the decrease of the free energy difference (Figure 3). Finally, we checked how membrane domain stability might affect the PMF profiles by simulating a less stable phase-separated membrane (DPPC/Chol/DUPC, Figure S1e).⁶ We obtained a much smaller free energy difference between the L_d and L_o domains (Figure 3), which is consistent with the different membrane partitioning thermodynamics of LAT in phase-separated giant unilamellar vesicles¹⁶ and giant plasma membrane vesicles.¹⁰ These results suggest that it is possible to obtain results with our method that are quantitatively comparable with experiments with further optimization of TMD packing density and other features and with the use of more complex lipid compositions.

Effects of TMD Physicochemical Properties on Membrane Orientation. As discussed above, raft affinity of TMDs is determined by protein–lipid interactions that are jointly regulated by the TMD hydrophobic length, hydrophobicity, size, and the lipid composition. Our approach using idealized model TMD provides a simple and fast means of predicting raft affinity. In addition to lateral dynamics, membrane orientation of TMD plays a critical role in regulating a variety of biological processes, such as switching of transmembrane proteins^{42–44} between active and inactive states. Our method can be used to quantify TMD membrane orientation. As shown in Figure 4, membrane orientation is affected by both the physicochemical properties of the TMD and the local lipid composition. In general, tilt angles are smaller when the TMDs are in the raft domain ($\Delta x < \sim 4.5$ nm) and the angle is seldom affected by the physicochemical properties of the TMD. When the TMD relocates to the nonraft domains, both hydrophobic mismatch and size significantly affect TMD tilt angles, particularly for the more hydrophobic TMDs. The effects of mismatch in the hydrophobic length are very obvious in all cases (Figure 4). When TMD hydrophobic length exceeds the hydrophobic thickness of the nonraft domains ($\Delta x > \sim 4.5$ nm), the tilt angle increases with hydrophobic length, which is consistent with the reported role of hydrophobic mismatch in TMD orientation.^{45–47} We further found that the mismatch in hydrophobicity between TMD and the hydrocarbon region of the membrane also has a dramatic impact on TMD orientation: more hydrophobic TMDs tend to have a larger tilt angle (Figure 4a,c). Furthermore, comparison of TMDs with $r = 0.6$ nm and $r = 1.2$ nm (Figure 4) clearly shows that the equilibrium tilt angle decreases with TMD radius.

CONCLUSIONS

In this work, we proposed an approach based on PMF calculations on idealized TMDs and model membranes to predict TMD membrane partitioning thermodynamics. By systematically varying the length, hydrophobicity, and size of our model TMDs and performing extensive umbrella sampling

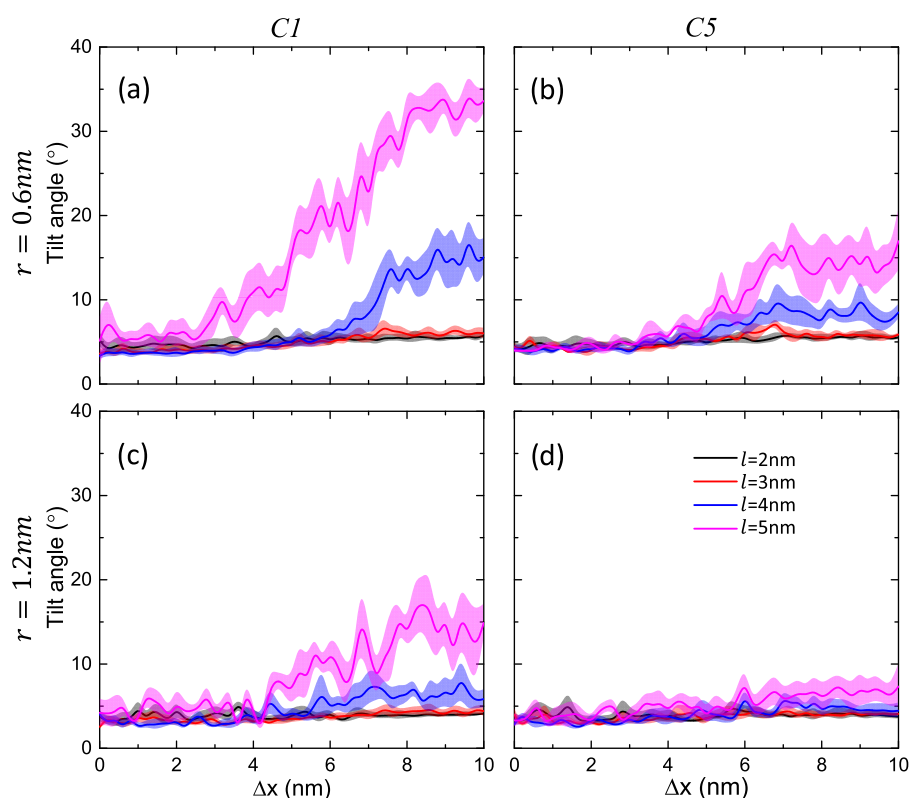


Figure 4. Average TMD tilt angle relative to the membrane normal, at different membrane localizations. Error bars are standard deviations using averaging over eight 100 ns blocks of the last 800 ns trajectory of each simulation and are shown as transparent shadows.

MD simulations, we showed that our method reproduced trends observed in experiments on the role of hydrophobic mismatch (mismatch in the hydrophobic length between TMD and the hydrocarbon region of membrane) in determining TMD raft affinity and orientation, which validated the feasibility of our approach. Our results further revealed a major impact of TMD hydrophobicity and size on raft affinity and membrane orientation, suggesting that lipid domain preference and orientation of TMDs are jointly determined by multiple physicochemical properties. It is worth mentioning that our calculations did not quantitatively reproduce lipid domain partitioning free energy of peptides such as LAT measured in giant plasma membrane vesicles. This is because, in addition to the many approximations inherent in CGMD, factors such as membrane domain stability, TMD flexibility, and roughness contribute to the lipid domain preference of proteins.

■ ASSOCIATED CONTENT

📄 Supporting Information

The Supporting Information is available free of charge on the ACS Publications website at DOI: [10.1021/acs.jpcc.8b10148](https://doi.org/10.1021/acs.jpcc.8b10148).

Initial TMD with $r = 0.6$ nm, $l = 4$ nm, and hydrophobicity “C1”; flexible and loosely packed TMD; top views of DPPC/Chol/DAPC and DPPC/Chol/DUPC; and side views of DPPC/Chol/DAPC (PDF)

■ AUTHOR INFORMATION

Corresponding Authors

*E-mail: linxbseu@buaa.edu.cn. Phone: +86-15510029836 (X.L.).

*E-mail: alemayehu.g.abebe@uth.tmc.edu. Phone: +1-7135007538 (A.A.G.).

ORCID

Xubo Lin: 0000-0002-4417-3582

Alemayehu A. Gorfe: 0000-0002-9328-4692

Notes

The authors declare no competing financial interest.

■ ACKNOWLEDGMENTS

We sincerely thank Prof. Ilya Levental for helpful discussion and anonymous reviewers for insightful comments. This work was supported by the National Institutes of Health Grant (R01GM100078) to A.A.G. and the 111 Project (B13003), the Fundamental Research Funds for the Central Universities, and the Startup Fund of Beijing Advanced Innovation Center to X.L. Computational resources were provided by the Texas Advanced Computing Center (TACC) and the Super-computer Center of Beihang University.

■ REFERENCES

- (1) Alberts, B. *Molecular Biology of the Cell*, 6th ed.; Garland Science: New York, 2017; pp 565–1021.
- (2) Nicolson, G. L. The Fluid—Mosaic Model of Membrane Structure: Still Relevant to Understanding the Structure, Function and Dynamics of Biological Membranes after More Than 40 years. *Biochim. Biophys. Acta, Biomembr.* **2014**, *1838*, 1451–1466.
- (3) Sezgin, E.; Levental, I.; Mayor, S.; Eggeling, C. The Mystery of Membrane Organization: Composition, Regulation and Roles of Lipid Rafts. *Nat. Rev. Mol. Cell. Biol.* **2017**, *18*, 361–374.
- (4) Veatch, S. L.; Keller, S. L. Miscibility Phase Diagrams of Giant Vesicles Containing Sphingomyelin. *Phys. Rev. Lett.* **2005**, *94*, No. 148101.

- (5) Goh, S. L.; Amazon, J. J.; Feigenson, G. W. Toward a Better Raft Model: Modulated Phases in the Four-Component Bilayer, Dspc/Dopc/Popc/Chol. *Biophys. J.* **2013**, *104*, 853–862.
- (6) Lin, X.; Lorent, J. H.; Skinkle, A. D.; Levental, K. R.; Waxham, M. N.; Gofre, A. A.; Levental, I. Domain Stability in Biomimetic Membranes Driven by Lipid Polyunsaturation. *J. Phys. Chem. B* **2016**, *120*, 11930–11941.
- (7) Lin, X.; Zhang, S.; Ding, H.; Levental, I.; Gofre, A. A. The Aliphatic Chain of Cholesterol Modulates Bilayer Interleaflet Coupling and Domain Registration. *FEBS Lett.* **2016**, *590*, 3368–3374.
- (8) Baumgart, T.; Hammond, A. T.; Sengupta, P.; Hess, S. T.; Holowka, D. A.; Baird, B. A.; Webb, W. W. Large-Scale Fluid/Fluid Phase Separation of Proteins and Lipids in Giant Plasma Membrane Vesicles. *Proc. Natl. Acad. Sci. U.S.A.* **2007**, *104*, 3165–3170.
- (9) Sezgin, E.; Kaiser, H.-J.; Baumgart, T.; Schwille, P.; Simons, K.; Levental, I. Elucidating Membrane Structure and Protein Behavior Using Giant Plasma Membrane Vesicles. *Nat. Protoc.* **2012**, *7*, 1042–1051.
- (10) Diaz-Rohrer, B. B.; Levental, K. R.; Simons, K.; Levental, I. Membrane Raft Association Is a Determinant of Plasma Membrane Localization. *Proc. Natl. Acad. Sci. U.S.A.* **2014**, *111*, 8500–8505.
- (11) Shah, A.; Chen, D.; Boda, A. R.; Foster, L. J.; Davis, M. J.; Hill, M. M. Raftprot: Mammalian Lipid Raft Proteome Database. *Nucleic Acids Res.* **2015**, *43*, D335–D338.
- (12) Lorent, J. H.; Diaz-Rohrer, B.; Lin, X.; Spring, K.; Gofre, A. A.; Levental, K. R.; Levental, I. Structural Determinants and Functional Consequences of Protein Affinity for Membrane Rafts. *Nat. Commun.* **2017**, *8*, No. 1219.
- (13) Lin, X.; Gofre, A. A.; Levental, I. Protein Partitioning into Ordered Membrane Domains: Insights from Simulations. *Biophys. J.* **2018**, *114*, 1936–1944.
- (14) Rose, P. W.; et al. The Rcsb Protein Data Bank: Integrative View of Protein, Gene and 3d Structural Information. *Nucleic Acids Res.* **2017**, *45*, D271–D281.
- (15) Lomize, M. A.; Pogozheva, I. D.; Joo, H.; Mosberg, H. I.; Lomize, A. L. Opm Database and Ppm Web Server: Resources for Positioning of Proteins in Membranes. *Nucleic Acids Res.* **2012**, *40*, D370–D376.
- (16) Shogomori, H.; Hammond, A. T.; Ostermeyer-Fay, A. G.; Barr, D. J.; Feigenson, G. W.; London, E.; Brown, D. A. Palmitoylation and Intracellular Domain Interactions Both Contribute to Raft Targeting of Linker for Activation of T Cells. *J. Biol. Chem.* **2005**, *280*, 18931–18942.
- (17) Levental, I.; Lingwood, D.; Grzybek, M.; Coskun, Ü.; Simons, K. Palmitoylation Regulates Raft Affinity for the Majority of Integral Raft Proteins. *Proc. Natl. Acad. Sci. U.S.A.* **2010**, *107*, 22050–22054.
- (18) Schäfer, L. V.; de Jong, D. H.; Holt, A.; Rzepiela, A. J.; de Vries, A. H.; Poolman, B.; Killian, J. A.; Marrink, S. J. Lipid Packing Drives the Segregation of Transmembrane Helices into Disordered Lipid Domains in Model Membranes. *Proc. Natl. Acad. Sci. U.S.A.* **2011**, *108*, 1343–1348.
- (19) de Jong, D. H.; Lopez, C. A.; Marrink, S. J. Molecular View on Protein Sorting into Liquid-Ordered Membrane Domains Mediated by Gangliosides and Lipid Anchors. *Faraday Discuss.* **2013**, *161*, 347–363.
- (20) Milovanovic, D.; Honigmann, A.; Koike, S.; Göttfert, F.; Pähler, G.; Junius, M.; Müller, S.; Diederichsen, U.; Janshoff, A.; Grubmüller, H.; et al. Hydrophobic Mismatch Sorts Snare Proteins into Distinct Membrane Domains. *Nat. Commun.* **2015**, *6*, No. 5984.
- (21) van Duyl, B. Y.; Rijkers, D. T.; de Kruijff, B.; Killian, J. A. Influence of Hydrophobic Mismatch and Palmitoylation on the Association of Transmembrane A-Helical Peptides with Detergent-Resistant Membranes. *FEBS Lett.* **2002**, *523*, 79–84.
- (22) Denny, P. W.; Field, M. C.; Smith, D. F. Gpi-Anchored Proteins and Glycoconjugates Segregate into Lipid Rafts in Kinetoplastida. *FEBS Lett.* **2001**, *491*, 148–153.
- (23) Wang, C.; Krause, M. R.; Regen, S. L. Push and Pull Forces in Lipid Raft Formation: The Push Can Be as Important as the Pull. *J. Am. Chem. Soc.* **2015**, *137*, 664–666.
- (24) Yue, T.; Li, S.; Zhang, X.; Wang, W. The Relationship between Membrane Curvature Generation and Clustering of Anchored Proteins: A Computer Simulation Study. *Soft Matter* **2010**, *6*, 6109–6118.
- (25) Hu, J.; Lipowsky, R.; Weikl, T. R. Binding Constants of Membrane-Anchored Receptors and Ligands Depend Strongly on the Nanoscale Roughness of Membranes. *Proc. Natl. Acad. Sci. U.S.A.* **2013**, *110*, 15283–15288.
- (26) Katira, S.; Mandadapu, K. K.; Vaikuntanathan, S.; Smit, B.; Chandler, D. Pre-Transition Effects Mediate Forces of Assembly between Transmembrane Proteins. *eLife* **2016**, *5*, No. e13150.
- (27) Schmidt, U.; Guigas, G.; Weiss, M. Cluster Formation of Transmembrane Proteins Due to Hydrophobic Mismatching. *Phys. Rev. Lett.* **2008**, *101*, No. 128104.
- (28) Periole, X.; Knepp, A. M.; Sakmar, T. P.; Marrink, S. J.; Huber, T. Structural Determinants of the Supramolecular Organization of G Protein-Coupled Receptors in Bilayers. *J. Am. Chem. Soc.* **2012**, *134*, 10959–10965.
- (29) Su, C.; Merlitz, H.; Rabbell, H.; Sommer, J. U. Nanoparticles of Various Degrees of Hydrophobicity Interacting with Lipid Membranes. *J. Phys. Chem. Lett.* **2017**, *8*, 4069–4076.
- (30) Sun, D.; Lin, X.; Gu, N. Cholesterol Affects C60 Translocation across Lipid Bilayers. *Soft Matter* **2014**, *10*, 2160–2168.
- (31) Risselada, H. J.; Marrink, S. J. The Molecular Face of Lipid Rafts in Model Membranes. *Proc. Natl. Acad. Sci. U.S.A.* **2008**, *105*, 17367–17372.
- (32) Marrink, S. J.; Risselada, H. J.; Yefimov, S.; Tieleman, D. P.; De Vries, A. H. The Martini Force Field: Coarse Grained Model for Biomolecular Simulations. *J. Phys. Chem. B* **2007**, *111*, 7812–7824.
- (33) Kästner, J. Umbrella Sampling. *Wiley Interdiscip. Rev.: Comput. Mol. Sci.* **2011**, *1*, 932–942.
- (34) Abraham, M. J.; Murtola, T.; Schulz, R.; Páll, S.; Smith, J. C.; Hess, B.; Lindahl, E. Gromacs: High Performance Molecular Simulations through Multi-Level Parallelism from Laptops to Supercomputers. *SoftwareX* **2015**, *1–2*, 19–25.
- (35) Bussi, G.; Donadio, D.; Parrinello, M. Canonical Sampling through Velocity Rescaling. *J. Chem. Phys.* **2007**, *126*, No. 014101.
- (36) Parrinello, M.; Rahman, A. Polymorphic Transitions in Single Crystals: A New Molecular Dynamics Method. *J. Appl. Phys.* **1981**, *52*, 7182–7190.
- (37) Ingólfsson, H. I.; Melo, M. N.; van Eerden, F. J.; Arnarez, C.; Lopez, C. A.; Wassenaar, T. A.; Periole, X.; De Vries, A. H.; Tieleman, D. P.; Marrink, S. J. Lipid Organization of the Plasma Membrane. *J. Am. Chem. Soc.* **2014**, *136*, 14554–14559.
- (38) Wimley, W. C.; White, S. H. Experimentally Determined Hydrophobicity Scale for Proteins at Membrane Interfaces. *Nat. Struct. Mol. Biol.* **1996**, *3*, 842–848.
- (39) Moon, C. P.; Fleming, K. G. Side-Chain Hydrophobicity Scale Derived from Transmembrane Protein Folding into Lipid Bilayers. *Proc. Natl. Acad. Sci. U.S.A.* **2011**, *108*, 10174–10177.
- (40) Quezada Gallo, J.-A.; Debeaufort, F.; Callegarin, F.; Voilley, A. Lipid Hydrophobicity, Physical State and Distribution Effects on the Properties of Emulsion-Based Edible Films. *J. Membr. Sci.* **2000**, *180*, 37–46.
- (41) Wang, C.; Yu, Y.; Regen, S. L. Lipid Raft Formation: Key Role of Polyunsaturated Phospholipids. *Angew. Chem., Int. Ed.* **2017**, *56*, 1639–1642.
- (42) Lelimosin, M.; Limongelli, V.; Sansom, M. S. Conformational Changes in the Epidermal Growth Factor Receptor: Role of the Transmembrane Domain Investigated by Coarse-Grained Metadynamics Free Energy Calculations. *J. Am. Chem. Soc.* **2016**, *138*, 10611–10622.
- (43) Seubert, N.; Royer, Y.; Staerk, J.; Kubatzky, K. F.; Moucadel, V.; Krishnakumar, S.; Smith, S. O.; Constantinescu, S. N. Active and Inactive Orientations of the Transmembrane and Cytosolic Domains

of the Erythropoietin Receptor Dimer. *Mol. Cell* **2003**, *12*, 1239–1250.

(44) Matsushita, C.; Tamagaki, H.; Miyazawa, Y.; Aimoto, S.; Smith, S. O.; Sato, T. Transmembrane Helix Orientation Influences Membrane Binding of the Intracellular Juxtamembrane Domain in Neu Receptor Peptides. *Proc. Natl. Acad. Sci. U.S.A.* **2013**, *110*, 1646–1651.

(45) Park, S. H.; Opella, S. J. Tilt Angle of a Trans-Membrane Helix Is Determined by Hydrophobic Mismatch. *J. Mol. Biol.* **2005**, *350*, 310–318.

(46) Kim, T.; Im, W. Revisiting Hydrophobic Mismatch with Free Energy Simulation Studies of Transmembrane Helix Tilt and Rotation. *Biophys. J.* **2010**, *99*, 175–183.

(47) Yeagle, P. L.; Bennett, M.; Lemaitre, V.; Watts, A. Transmembrane Helices of Membrane Proteins May Flex to Satisfy Hydrophobic Mismatch. *Biochim. Biophys. Acta, Biomembr.* **2007**, *1768*, 530–537.